

SUMMARY OF AN ASSESSMENT OF JEF2.2 NUCLEAR DATA LIBRARY FOR LWR  
LATTICE CALCULATIONS

D Hanlon  
N T Gulliford

Experimental Reactor Physics Department  
Safety And Performance Division  
Winfrith Technology Centre

June 1993

14090261

## 1 INTRODUCTION

The Joint Evaluated File (JEF) of basic nuclear data is being established as the European standard for performance and safety calculations throughout the fuel cycle. Benchmark experiments performed in the DIMPLE reactor are included in the JEF International Integral Benchmark Testing Programme. One such series of experiments is the DIMPLE S06 Cruciform Assembly Lattice Study that was undertaken to validate the reactor physics calculation methods and data used in the design and operation of thermal power reactors. The programme extended previous studies in water reflected cylindrical systems to power reactor geometries by assembling a cruciform array of 3% enriched uranium dioxide fuel pins. The array simulated the rectangular corner configuration of a Pressurised Water Reactor (PWR) and effectively represented twelve PWR fuel assemblies.

Three primary versions of the cruciform assembly were constructed, the first (S06A) being water reflected as with the cylindrical systems. The cruciform assembly was then surrounded azimuthally by a stainless steel reflector to evaluate the impact of a typical PWR baffle region (S06B). The S06A and S06B experiments concentrated on the measurement of pin powers at the complex radial core/reflector boundary, where it is important to quantify the accuracy of predictions for both fuel management operations and ex-core surveillance procedures.

The third version of the cruciform assembly (S06C) investigated the effect of discrete burnable poison pins and empty guide thimbles on reaction-rate distributions and their prediction. The burnable poison pins were of the type used in many current PWRs, comprising stainless steel clad annuli of borosilicate glass. Configurations ranged from a single isolated poison pin, through a central complex cluster that included simulated empty guide thimbles, to distributed poison arrays adjacent to the surrounding baffle. An asymmetric absorber loading was also designed to provide a 25% power tilt across the cruciform assembly.

A range of core physics parameters, such as the critical moderator level and water height reactivity coefficient, was measured in each assembly. Extensive reaction-rate distribution measurements and diagnostic  $^{235}\text{U}$  fission fine structure measurements through a fuel pin, discrete burnable poison pin and simulated empty guide thimble were performed to provide detailed data for the assessment of the accuracy of pin power predictions.

Throughout the experimental programme, data were published in a series of DIMPLE Technical Notes and interim results were presented at a number of conferences<sup>1-3</sup>. A final report provided a thorough specification of the DIMPLE S06 series of configurations in a benchmark format suitable for independent analysis<sup>4</sup>. In addition, the cruciform assemblies were calculated in a consistent manner using the LWRWIMS lattice code and its associated WIMS86 nuclear data library. Reference 4 therefore also provides a detailed comparison of the experimental results and the predictions.

This report provides the first assessment of the latest JEF2.2 library release using the DIMPLE S06 Cruciform Assembly Lattice Study. The geometric models established for the

14090262

previous WIMS86 calculations have been employed in the JEF2.2 library calculations, allowing a direct comparison of the processed libraries. This report compares the k-effective values and whole core reaction-rate distributions calculated using both libraries with the benchmark measurements.

## 2 THE MEASUREMENTS

### 2.1 Brief Description of DIMPLE

DIMPLE is one of two low power reactors owned and managed by the AEA at its Winfrith site in the South of England. The reactors offer a comprehensive research capability<sup>5</sup>.

DIMPLE is a versatile, water moderated reactor used to investigate performance, safety and safeguards issues relevant to the entire nuclear fuel cycle. Thus, in addition to the lattice studies described in this report, the current DIMPLE programme includes reactivity and neutron source measurements with samples of irradiated fuel discharged from power reactors,<sup>6</sup> criticality experiments relevant to fuel manufacturing, transport, storage and reprocessing issues,<sup>7</sup> and the development of sub-critical monitoring techniques.<sup>8</sup>

The reactor can accommodate a wide range of experimental configurations. Conventional assemblies consist of fuel pins supported, and precisely located, between upper and lower lattice plates inside a large aluminium primary vessel (2.6m diameter and 4m high). Both simple geometry fuel pin benchmarks and more complex configurations, representative of operational or accident conditions, can be built. Flexibility is accomplished by varying the lattice plate design, fuel type and the inclusion of non-fuel components such as structural or absorber materials. Designs have been investigated for other fuel geometries (eg plate fuel and solutions) and systems with neutron spectra ranging from fast to well thermalised. The ability to control the reactor by means of moderator level alone permits sub-critical and critical assemblies to be studied without the complicating perturbation of control rods. Shutdown is achieved by means of a fast-dump system. When the reactor is operating, a 2m diameter stainless steel bell-jar situated approximately 25cm below the core sustains an air cavity. By venting the cavity through a pair of large valves, the water level can be dropped by 30cm in about one second.

The reactor's low power operation of less than 200W and ease of access provides for efficient configuration modifications or complete assembly changes.

### 2.2 The Experimental Assemblies

The S06 series of configurations, summarised in Table 1, was based on a cruciform array of 3072 fuel pins on a 1.2507cm square pitch. As shown in Figure 1, this simulated the rectangular corner configuration of a PWR and effectively represented twelve PWR assemblies. Only the radial core boundary differed between the first two assemblies, with S06A (Figure 2) having a fuel pin/water reflector boundary and S06B (Figure 3) having a 2.67cm thick stainless steel baffle region between the core and water region. This baffle made S06B and subsequent assemblies more representative of the Sizewell PWR configuration. The inner edge of the baffle was located one-half pitch from the centres of the outermost pins.

The S06C study involved a series of discrete burnable poison pin arrays within the cruciform baffle assembly. Measurements were concentrated on the S06C/0 reference assembly and the three key burnable poison configurations of the central array (S06C/8), the symmetric distributed array (S06C/10) and the asymmetric version (S06C/11).

The fuel pins consisted of sintered 3% enriched uranium dioxide pellets, wrapped in adhesive aluminium foil and stacked within stainless steel cans to a fuel height of approximately 69cm. The design of the discrete burnable poison pin used in the S06C configurations was based on the type proposed for Sizewell-B and comprised stainless steel clad annuli of borosilicate glass (pyrex) with a natural boron content of 4%. Moderator-filled vacant fuel pin locations were used to simulate empty guide thimbles and control overall reactivity. To accommodate the S06C range of different poison pin arrays, the eight outer simulated PWR assemblies of S06B were each modified to include five moderator locations.

Reference 4 provides a detailed specification of the geometry and composition data necessary to perform 2-dimensional and 3- dimensional calculations, together with their associated uncertainties.

### 2.3 Characterization of the Assemblies

In addition to the detailed definition of geometry and composition, the characterization of the S06 series of assemblies involved the measurement of a range of core physics parameters. For each assembly, the critical moderator level and the water height reactivity coefficient ( $d/dH$ ) were determined experimentally.

Comprehensive axial and radial reaction-rate distributions were measured in S06A, S06B and four key configurations in the S06C series (S06C/0, S06C/8, S06C/10 and S06C/11) to provide detailed data for comparison with calculated values. Included were three reactions of major significance to the overall neutron balance, namely fission in  $^{235}\text{U}$  and  $^{238}\text{U}$  and capture in  $^{238}\text{U}$ , as well as fission in  $^{239}\text{Pu}$ . Relative radial reaction-rate scans were performed with activation foils located at the plane of the peak axial flux. Axial measurements were carried out with foils at a central core location and, more extensively, with a miniature fission chamber.

To relate the distributions measured for each reaction, experiments were performed at a central core location to determine the  $^{238}\text{U}$  to  $^{235}\text{U}$  Fast Fission Ratio (FFR), the  $^{239}\text{Pu}$  to  $^{235}\text{U}$  fission ratio and the Relative Conversion Ratio (RCR). In the context of this work the RCR is defined as the ratio of the capture-rate per atom of  $^{238}\text{U}$  to the fission-rate per atom of  $^{235}\text{U}$  in the DIMPLE core, relative to the corresponding ratio measured in the well-defined thermal column spectrum of the NESTOR neutron source reactor.

An important feature of the S06C phase of the experimental programme was the measurement of the  $^{235}\text{U}$  fission fine structure through a fuel pin, burnable poison pin and simulated empty guide thimble. These experiments were designed to provide detailed diagnostic data to supplement the results of whole assembly reaction-rate distribution measurements.

Descriptions of the critical moderator height and  $d/dh$  measurements, the axial fission chamber measurements, the whole assembly relative reaction-rate foil measurements, the absolute reaction-rate ratio measurements and the  $^{235}\text{U}$  fission fine structure measurements can be found in Reference 4.

### 3 CALCULATIONS

The six key DIMPLE S06 benchmarks were first calculated in a consistent manner using the LWRWIMS lattice code (Version 2B) and its associated WIMS86 data library<sup>9</sup>. The calculations have been repeated here with a new 172-group nuclear data library generated from the JEF2.2 source library using the NJOY89.62W processing code package<sup>10</sup>. The current release of the LWRWIMS lattice code (Version 3A) was employed in these calculations, where the differences with Version 2B are in the editing options and do not affect the comparison of the WIMS86 and JEF2.2 data-sets. Reference 11 provides an overview of the main capabilities of LWRWIMS, where for power reactor calculations the package is used to generate data for the three-dimensional steady state, transient and fuel management code PANTHER.<sup>12</sup>

The JEF2.2 assessment calculations were performed using the identical geometric models and composition data employed in the WIMS86 calculations<sup>4</sup>. A quarter plan model of the basic cruciform assembly was constructed on a 39 x 39 mesh grid, with meshes 1 to 35 being one pin pitch in width and 36 to 39 in the radial reflector being about two pin pitches. Each mesh was occupied by a cell type representing a fuel pin, poison pin, moderator or baffle region, with the pin cells specified as annular regions surrounded by moderator. Cell types of the same geometry and composition were defined as different when located near regions that could affect the calculation of cross-sections. The quarter plan model was used for all but the asymmetric S06C/11 configuration, where a half plan model was necessary.

Within the LWRWIMS framework, macroscopic cross-sections were calculated using the new JEF2.2 172 energy group data library. In the code package, collision probabilities are calculated for each cell type, with individual cell probabilities coupled using a multicell method that ensures a consistent interaction treatment. The cross-section data were generated for the different cell types in each of the S06 models in a smeared pin form for a GOG diffusion calculation. These cross-sections were produced in both the standard WIMS 69 energy groups and the 6-group structure recommended for Sizewell-B, with boundaries at 0.821MeV, 9.118keV, 4.00eV, 0.625eV and 0.140eV.

For calculations involving poison pins and empty guide thimbles, experience has shown that the simple combination of pin cell smearing and finite difference diffusion theory leads to insufficiently accurate reaction-rate distributions. The CACTUS DMOD option<sup>11</sup> was therefore used to derive modified diffusion coefficients. CACTUS employs a characteristics solution of the differential transport equation in the unsmeared pin-cell geometry. This provides a method for deriving effective diffusion coefficients for lattice heterogeneities that makes allowance for transport to diffusion differences, pin-cell smearing and finite difference effects. Problems were encountered for S06C/8 and S06C/11 using this option in JEF2.2 calculations involving

large numbers of groups (ie 172-groups and 69-groups). Whilst the GOG k-effective values appeared unaffected, the CACTUS-DMOD k-values failed to converge within the maximum number of iterations and produced large over-predictions of the  $^{235}\text{U}$  fission-rate within the simulated empty guide thimble meshes. Only the reaction-rate distributions calculated using the 6-group energy scheme have therefore been compared with the measured values. For the same reason, comparisons of the measured and calculated  $^{235}\text{U}$  fission fine structure cannot be carried out until the problem with large group JEF2.2 calculations has been resolved.

The axial leakage in the whole assembly calculations was represented by applying a buckling term derived from the axial fission-rate measurements. The calculations employed the BZERO option recommended for high leakage situations, where the buckling dependent correction factors used the values input after the BUCKLINGS keyword.

Both 69-group and 6-group calculations were performed for each of the key benchmarks to a convergence equivalent to 0.0001 (-1/k).

## 4 COMPARISON OF THE MEASUREMENTS AND CALCULATIONS

### 4.1 k-effective Values

The k-effective values calculated by LWRWIMS for the six key S06 assemblies are presented in Table 2. In every case k-effective is underpredicted, with mean differences from unity of  $-0.0023 \pm 0.0010$  (-1/k) and  $-0.0029 \pm 0.0008$  (-1/k) for the 69-group and 6-group calculations, respectively. Relative to the overall experimental uncertainty of  $\pm 0.001$ , these differences are at about the three-sigma level. The JEF2.2 k-effective values are a significant improvement on the WIMS86 mean differences of  $-0.0076 \pm 0.0006$  (-1/k) and  $-0.0096 \pm 0.0008$  (-1/k) for the 69-group and 6-group calculations, respectively.

As in other reactor physics codes, it is assumed in LWRWIMS that all neutrons are born at energies in the prompt neutron fission spectrum. In reality, a small fraction (~0.7%) are born in the delayed neutron spectrum at slightly lower energies. Calculations to assess the importance of this effect on k-effective indicate the correction is only +0.0002 for the S06 assemblies<sup>14</sup>.

### 4.2 Reaction-Rate Distributions

Detailed tabulations comparing the measured  $^{235}\text{U}$  fission,  $^{239}\text{Pu}$  fission,  $^{238}\text{U}$  fission and  $^{238}\text{U}$  capture radial distribution results with the values calculated using the 6-group WIMS86 and JEF2.2 data libraries are given in Reference 15 for each of the key configurations.

The impact of the radial boundary on the cruciform assembly power distribution is demonstrated in Figures 2 and 3, where the measured and calculated  $^{235}\text{U}$  fission-rates are plotted along the central radial axes and core boundaries for S06A and S06B, respectively.

The marked difference in the S06B distribution relative to that for S06A is due to the baffle preventing neutrons thermalised in the water reflector from re-entering the core and enhancing fission in the outer-most pins. Figure 2 indicates a significant improvement in the predicted  $^{235}\text{U}$  fission-rate using the JEF2.2 library.

Over two and a half thousand foil measurements were performed during the S06 series and, to assist assimilation of comparisons with the predicted reaction-rates, mean C/E values have been derived for the same representative regions in each assembly. These six regions are identified in the S06A calculation model shown in Figure 4. The mean C/E values and associated standard errors are summarised in Table 3 for the 6-group JEF2.2 and WIMS86 calculation models, respectively.

Each of the four reaction-rate distribution results predicted for S06A using the JEF2.2 library are lower than those calculated using the current WIMS86 library, with the difference relative to the normalisation positions increasing to around 5% in the outermost row of pins.

For the S06B and S06C assemblies, where the stainless steel baffle prevented neutrons thermalised in the water reflector from re-entering the core, the situation is somewhat different. The JEF2.2 reaction-rates are still generally lower than the WIMS86 results, although to a lesser degree, with the exception of the  $^{235}\text{U}$  and  $^{239}\text{Pu}$  fission-rates in the outermost row of pins where the JEF2.2 values are 1-2% higher. In comparison with the measured reaction-rate distributions, the performance of the two sets of 6-group calculations is broadly similar.

#### 4.3 Reaction-Rate Ratios

The results from the absolute reaction-rate ratio measurements performed at the centre of S06B are compared with the whole assembly GOG calculated values in Table 4. The measured  $^{239}\text{Pu}$  to  $^{235}\text{U}$  fission ratio and the  $^{238}\text{U}$  capture to  $^{235}\text{U}$  fission ratio have been derived using Maxwellian averaged thermal cross-sections calculated with the appropriate data library.

The C/E values based on the 6-group JEF2.2 model for  $^{238}\text{U}$  fission,  $^{239}\text{Pu}$  fission and  $^{238}\text{U}$  capture relative to  $^{235}\text{U}$  fission at the centre of S06B are  $0.961 \pm 0.034$ ,  $0.997 \pm 0.009$  and  $0.985 \pm 0.005$ , respectively. In each case experiment and prediction agrees within the experimental uncertainties.

### 5 CONCLUSIONS

Six key configurations studied during the DIMPLE S06 cruciform assembly programme have been calculated in a consistent manner using the current release of the LWRWIMS lattice code and a new JEF2.2 processed nuclear data library. The cross-section data were generated in a 6-group smeared pin form for GOG diffusion calculations, with modified diffusion coefficients derived using the CACTUS-DMOD option for the cases involving singularities. A problem in the use of large group schemes with CACTUS-DMOD calculations was identified and has yet to be resolved. The calculated k-effective values are consistently slightly

underpredicted, with the mean difference from unity being at about the three-sigma level of the experimental uncertainty.

Comparison of the new library with the current WIMS86 library shows a general tendency for the JEF2.2 values to be lower for  $^{235}\text{U}$  fission,  $^{239}\text{Pu}$  fission,  $^{238}\text{U}$  fission and  $^{238}\text{U}$  capture throughout the assemblies. However, for the assemblies surrounded by a baffle region, the JEF2.2 calculations are 1-2% higher at the outermost pin positions for  $^{235}\text{U}$  and  $^{239}\text{Pu}$  fission. In comparison with the measured reaction-rate distributions, the performance of the two sets of 6-group calculations is broadly similar.

The results of this study have provided confidence in the JEF2.2 source library and in the processing route employed to produce the LWRWIMS data library. The results of the assessment will be assimilated into the JEF International Integral Benchmark Testing Programme.

14090268



## REFERENCES

- 1 A. D. KNIPE, B. L. H. BURBIDGE and B. M. FRANKLIN  
Core/Reflector Boundary Studies in DIMPLE  
Proc. Int. Reactor Physics Conf., Jackson Hole, Wyoming,  
September 18-22, 1988, III, 465-476 (1988).
- 2 A. D. KNIPE, P. C. MILLER, K. G. GREENHOUSE and  
M. F. MURPHY  
The Use of a DIMPLE Mock-up Experiment to Assess the  
Uncertainties in the Radial Shield Fluxes of a PWR  
Proc. 7th Int. Conf. Radiation Shielding, Bournemouth,  
September 12-16, 1988, I, 231-239, (1988).
- 3 A. D. KNIPE, B. L. H. BURBIDGE and B. M. FRANKLIN  
A Burnable Poison Pin Benchmark Study in DIMPLE  
Proc. Int. Conf. Physics of Reactors: Operation, Design  
and Computation, Marseille, April 23-27, 1990, 1, IV, 1-12,  
(1990).
- 4 A. D. KNIPE, B. M. FRANKLIN, B. L. H. BURBIDGE,  
M. F. MURPHY, A. S. DAVIES and D. HANLON  
The DIMPLE Cruciform Assembly Benchmark Series  
AEA Report AEA-RS-1072, April 1991
- 5 A. D. KNIPE  
Status of UKAEA Low Power Reactors  
Proc. Int. Top. Mtg. Safety, Status and Future of Non-Commercial Reactors and  
Irradiation Facilities, Boise, Idaho, Sept 30 - Oct 4, 1990, 223-230, (1990).
- 6 J. MARSHALL, G. INGRAM, N. T. GULLIFORD and M. DARKE  
Irradiated Fuel Measurements in DIMPLE  
Proc. Int. Conf. Physics of Reactors: Operation, Design  
and Computation, Marseille, April 23-27, 1990, 2, XI, 45-54, (1990).
- 7 J. M. STEVENSON, B. M. FRANKLIN, B. L. H. BURBIDGE,  
A. PRESCOTT and G. POULLOT  
Loading Accident with Fuel Elements of Unequal Reactivity  
EUR-12048-EN, Commission of the European Communities (1989).
- 8 G. INGRAM, A. D. KNIPE and B. M. FRANKLIN  
Development of Subcritical Monitoring Techniques Using the DIMPLE Reactor  
Proc. Int. Topl. Mtg. Safety Margins in Criticality Safety, San Francisco, California,  
November 26-30, 1989, 104-111, (1989).

- 9 M. J. HALSALL and C. J. TAUBMAN  
The '1986' WIMS Nuclear Data Library  
AEA Report AEEW-R2133, (1986).
- 10 R. J. Perry and C. J. Dean  
JEF2.2 Benchmark Calculations for Thermal Reactor Pincells  
using WIMS at Winfrith  
JEF/DOC/395 (1993)
- 11 M. J. HALSALL, D. POWNEY and M. R. MOXOM  
LWRWIMS, The WIMS Code for Light Water Reactors  
Proc. Int. Conf. Physics of Reactors: Operation, Design and Computation,  
Marseille, April 23-27, 1990, IV, 45-55, (1990).
- 12 J. C. A. EMMETT and P. K. HUTT  
PANTHER and the UK Code Package for Fuel Management Calculations  
IAEA Technical Committee on Improvements of In-Core Fuel Management Codes,  
Madrid, July 12-15, 1988.
- 13 W. A. V. BROWN, et al  
Measurements of Material Buckling and Detailed Reaction Rates in a Series of Low  
Enrichment  $\text{UO}_2$  Fuelled Cores Moderated by Light Water  
AEA Report AEEW-R502, (1967).
- 14 N. T. GULLIFORD  
Influence of Delayed Neutron Importance on the Calculated Reactivity for Thermal  
Systems  
AEA Report AEA-RS-1183, (1993)
- 15 D. HANLON  
Assessment of JEF2.2 Nuclear Data Library for LWR Lattice Calculations  
AEA Report AEA-RS-1253, (1993)

**Table 1**  
**Summary of the DIMPLE S06 Cruciform Assemblies**

Assembly	Description
S06A	Cruciform assembly without baffle (3072 fuel pins simulating 12 PWR assemblies)
S06B	Cruciform assembly with baffle
S06C/0	S06C series reference (S06B with 40 water meshes in 8 outer simulated PWR assemblies)
S06C/1	4 isolated burnable poison pins at corners of central 16x16 array
S06C/2	8 burnable poison pins (central outer ring)
S06C/3	8 burnable poison pins + 4 water meshes (central outer ring)
S06C/4	8 burnable poison pins (central inner ring)
S06C/5	8 burnable poison pins + 4 water meshes (central inner ring)
S06C/6	4 burnable poison pins at central inner ring water mesh locations of S06C/5
S06C/7	12 burnable poison pins (central inner ring) ie S06C/4+S06C/6
S06C/8	16 burnable poison pins + 8 water meshes (central inner and outer rings) ie S06C/3+S06C/5
S06C/9	8 water meshes in central inner and outer rings
S06C/10	4 burnable poison pins in each of 8 outer simulated PWR assemblies
S06C/11	4 burnable poison pins in each of 4 adjacent outer simulated PWR assemblies (asymmetric configuration)

**Table 2**

**Calculated k-effective Values for the Key S06 Assemblies**

Assembly	k-effective			
	WIMS86		JEF2.2	
	69-Group	6-Group	69-Group	6-Group
S06A	0.9926	0.9916	0.9972	0.9974
S06B	0.9927	0.9905	0.9986	0.9976
S06C/0	0.9930	0.9909	0.9987	0.9980
S06C/8	0.9915	0.9895	0.9961	0.9957
S06C/10	0.9927	0.9904	0.9982	0.9972
S06C/11	0.9920	0.9898	0.9973	0.9968

**Table 3****Mean Whole Assembly Reaction-Rate C/E Values (6-Group JEF2.2 Calculation Model)**

Reaction	Zone 6	Zone 5	Zone 4	Zone 3	Zone 2	Zone 1
<b>S06A</b>						
<sup>235</sup> U Fission	0.996±0.003	0.994±0.001	0.985±0.003	0.972±0.003	0.977±0.004	0.994±0.002
<sup>239</sup> Pu Fission	0.991±0.003	0.990±0.004	0.980±0.001	0.973±0.003	0.978±0.001	1.005±0.002
<sup>238</sup> U Fission	0.993±0.004	0.987±0.006	0.981±0.006	0.973±0.005	0.932±0.007	0.852±0.011
<sup>238</sup> U Capture	0.994±0.004	0.993±0.005	0.979±0.004	0.982±0.005	0.965±0.004	0.983±0.004
<b>S06B</b>						
<sup>235</sup> U Fission	0.997±0.002	0.996±0.004	0.993±0.002	0.986±0.006	0.986±0.002	1.044±0.005
<sup>239</sup> Pu Fission	0.994±0.002	0.992±0.001	0.984±0.001	0.979±0.003	0.981±0.003	1.022±0.005
<sup>238</sup> U Fission	0.996±0.003	1.000±0.012	0.996±0.004	0.972±0.003	0.967±0.009	0.942±0.007
<sup>238</sup> U Capture	1.008±0.002	1.001±0.010	0.990±0.004	0.979±0.007	0.977±0.006	0.982±0.004
<b>S06C/0</b>						
<sup>235</sup> U Fission	1.009±0.005	1.010±0.007	1.011±0.000	0.989±0.004	0.993±0.008	1.045±0.007
<b>S06C/8</b>						
<sup>235</sup> U Fission	1.006±0.002	1.007±0.006	1.016±0.005		1.005±0.005	
<sup>239</sup> Pu Fission	1.006±0.003	1.001±0.002	1.005±0.003		0.997±0.005	
<sup>238</sup> U Fission	0.999±0.003	1.002±0.003	0.997±0.016		0.971±0.012	
<sup>238</sup> U Capture	1.017±0.002	1.004±0.003	1.026±0.009		0.999±0.007	
<b>S06C/10</b>						
<sup>235</sup> U Fission	1.002±0.002	1.000±0.004	1.006±0.002	0.988±0.006	0.991±0.005	1.044±0.005
<sup>239</sup> Pu Fission	1.001±0.002	1.000±0.004	1.001±0.002	0.987±0.005	0.992±0.003	1.028±0.003
<sup>238</sup> U Fission	1.001±0.003	1.000±0.006	0.998±0.003	0.994±0.004	0.976±0.007	0.951±0.006
<sup>238</sup> U Capture	0.999±0.003	0.998±0.003	1.006±0.001	0.992±0.006	0.986±0.003	1.001±0.002
<b>S06C/11</b>						
<sup>235</sup> U Fission	0.999±0.001	1.002±0.004	1.005±0.003	0.980±0.004	0.987±0.006	1.020±0.007

14090273

**Table 4**

**Comparison of Absolute Reaction-Rate Ratio Measurements and 6-group calculations in DIMPLE Assembly S06B**

Data Library	F8/F5			F9/F5			C8/F5		
	Measurement	Calculation	C/E	Measurement	Calculation	C/E	Measurement	Calculation	C/E
JEF2.2	0.00343±3.4%	0.00329	0.961±0.034	2.324±0.9%	2.318	0.997±0.009	0.0238±0.5%	0.02345	0.985±0.005
WIMS86	0.00343±3.4%	0.003385	0.987±0.034	2.274±0.9%	2.267	0.997±0.009	0.0236±0.5%	0.02344	0.993±0.005

14C90274

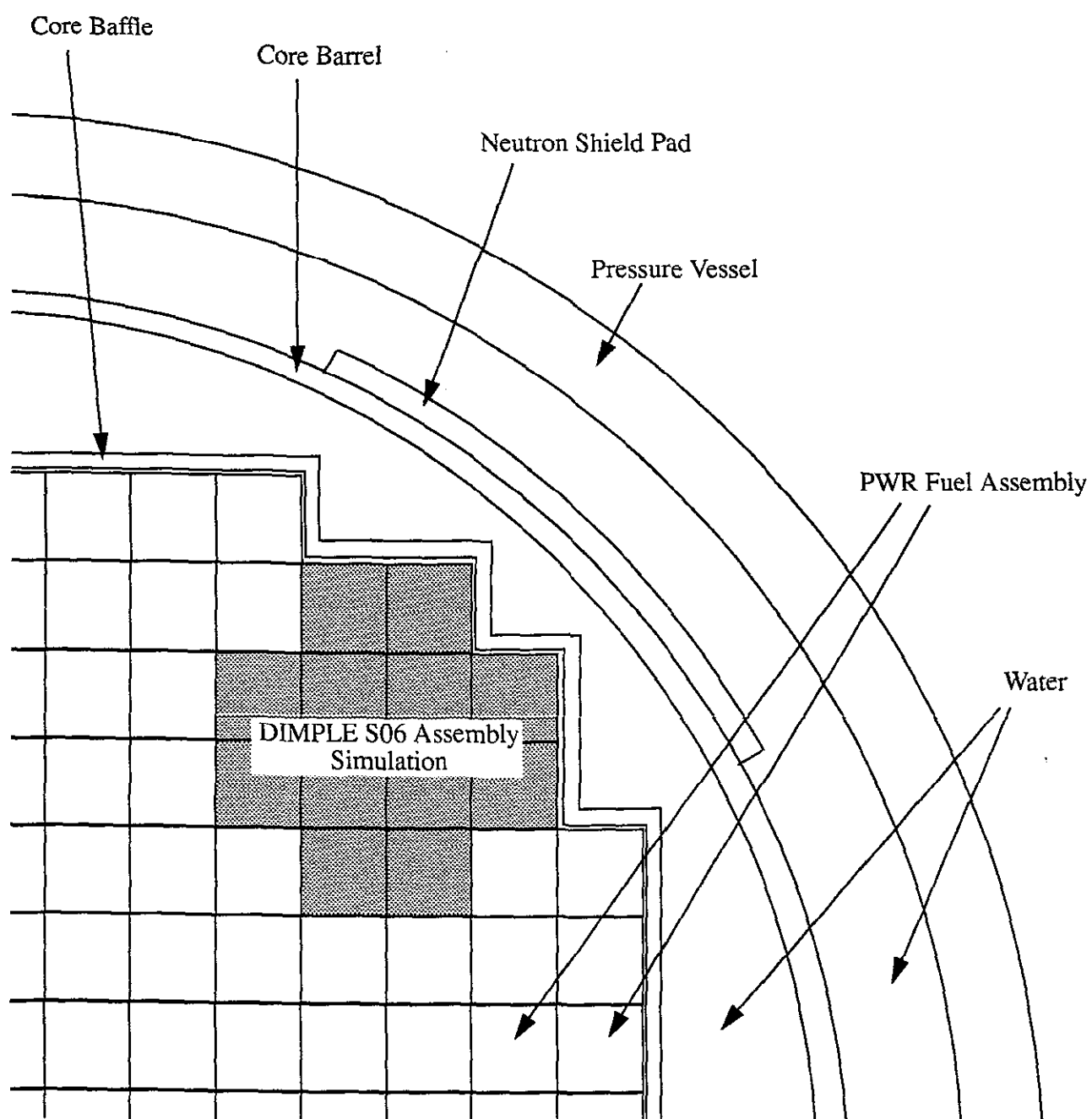


Figure 1 Sectional View Within Quadrant of PWR Pressure Vessel Showing DIMPLE S06 Assembly Simulation

14C90275

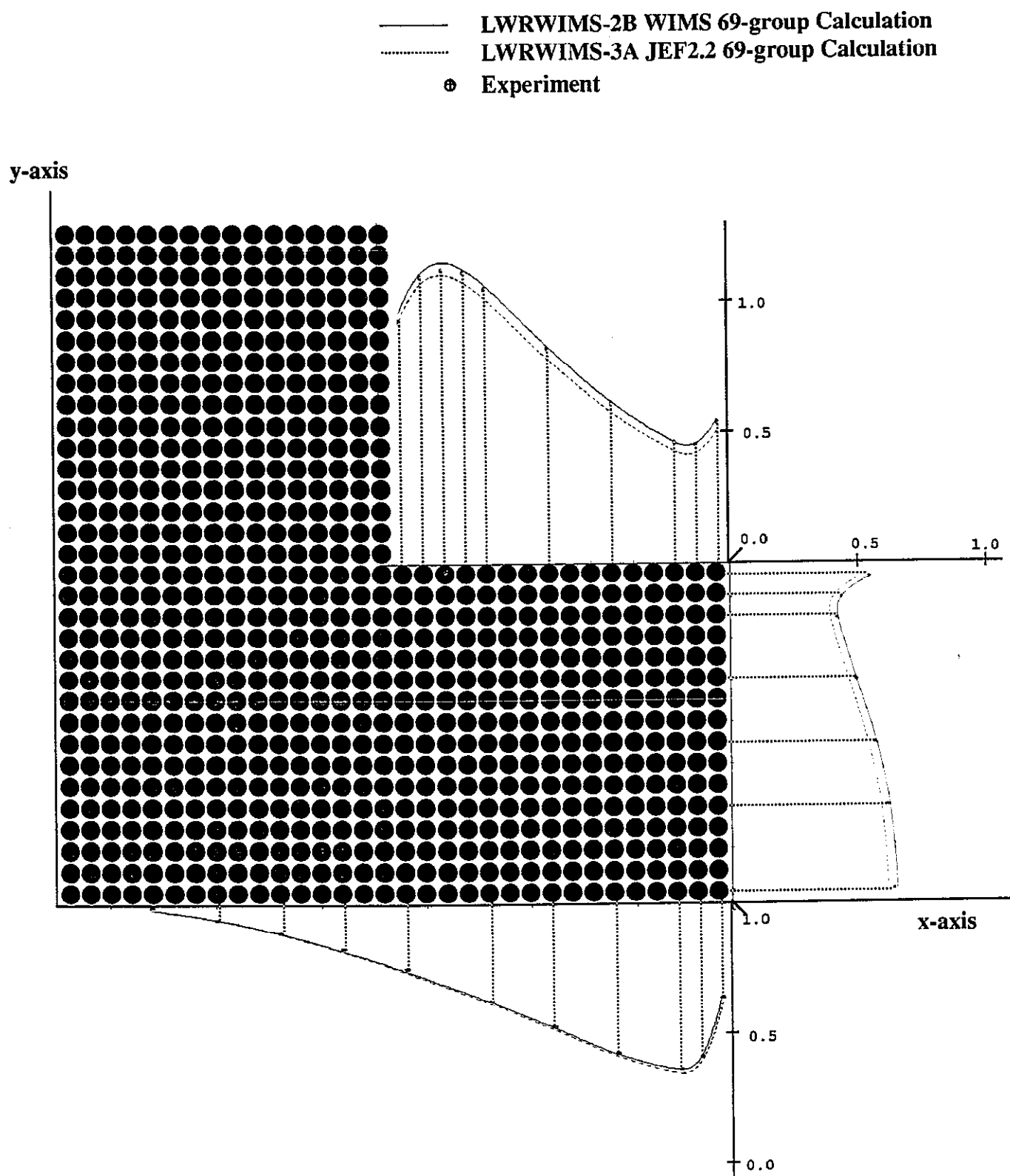


Figure 2. The  $^{235}\text{U}$  Fission Distribution in Assembly S06A

14C90276



— LWRWIMS-2B WIMS 69-group Calculation  
 ..... LWRWIMS-3A JEF2.2 69-group Calculation  
 ⊕ Experiment

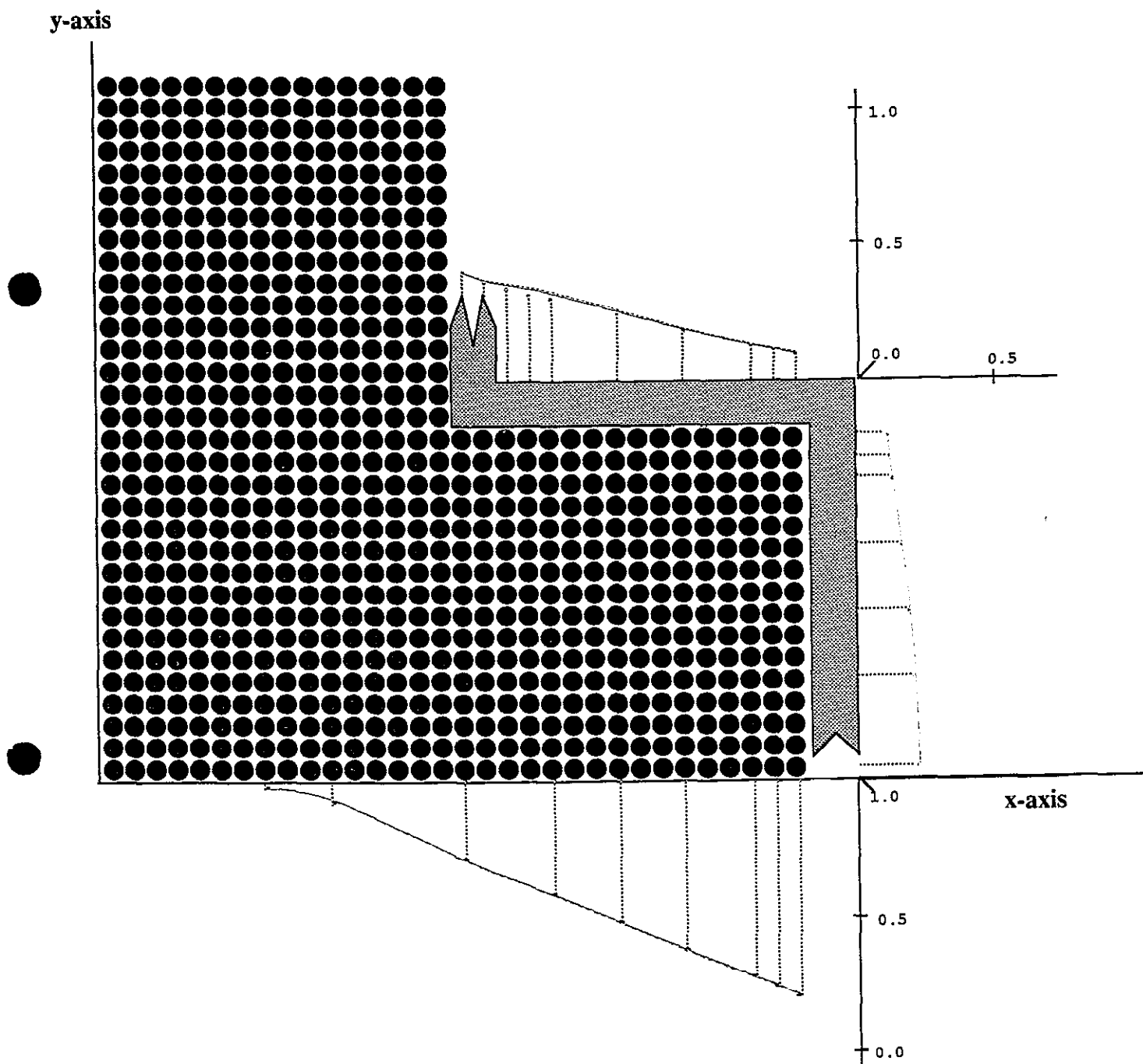


Figure 3. The  $^{235}\text{U}$  Fission Distribution in Assembly S06B

14090277

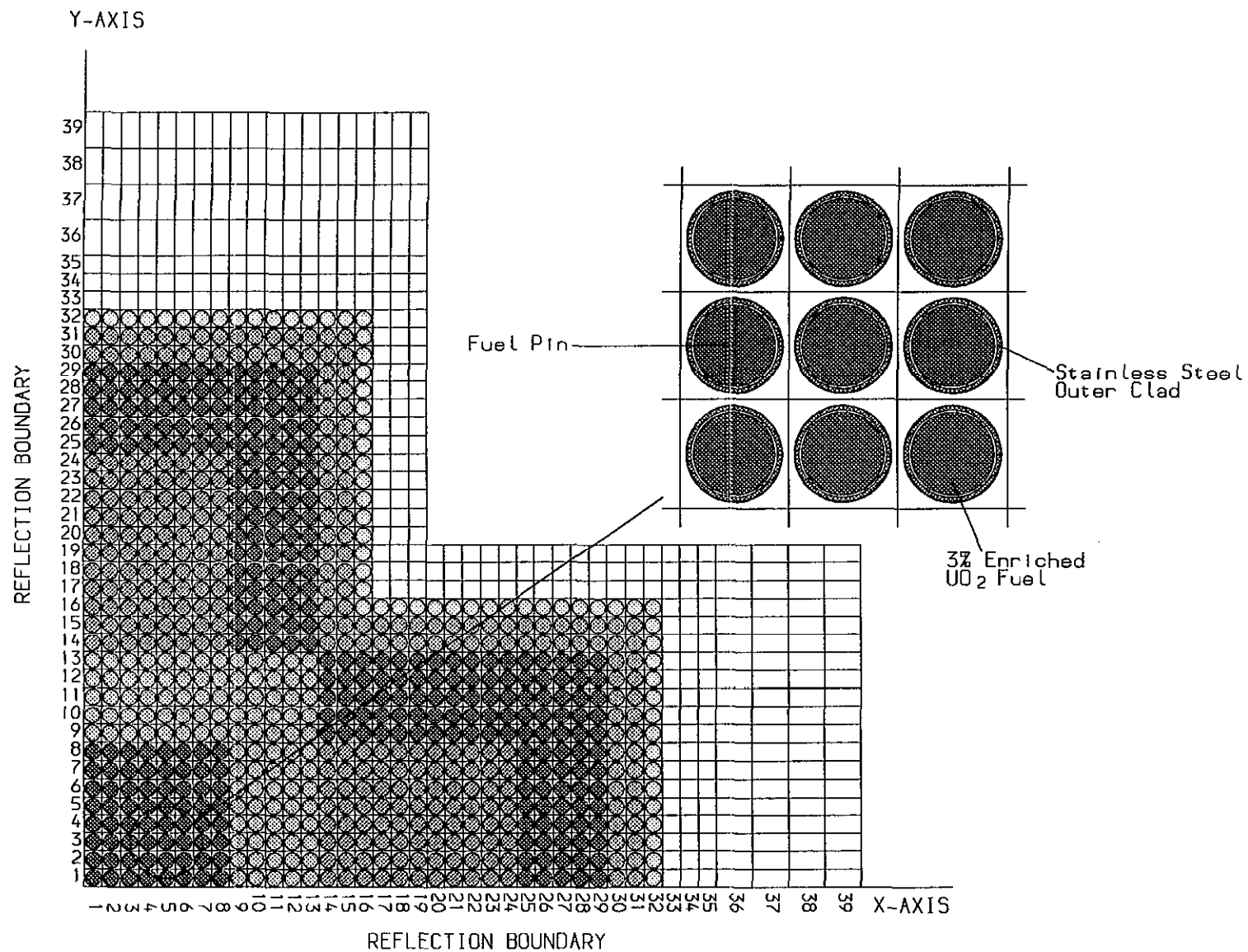


FIGURE 4 CALCULATION MODEL FOR DIMPLE ASSEMBLY S06A

14090270